Friction **5**(1): 108–114 (2017)
DOI 10.1007/s40544-017-0148-8
ISSN 2223-7690
CN 10-1237/TH
RESEARCH ARTICLE

Tribology behavior on scratch tests: Effects of yield strength

Biao FENG[*,†]

Department of Aerospace Engineering, Iowa State University, Ames, Iowa 50011, USA

[†] *Present address: Theoretical Division, Los Alamos National Laboratory, Los Alamos, New Mexico 87544, USA*

Received: 04 October 2016 / Revised: 16 November 2016 / Accepted: 11 January 2017

Abstract: A three-dimensional (3D) scratch model is proposed to investigate the effects of yield strength of both coatings and substrates. With the help of combined Coulomb and plastic friction, the obtained results comprehensively interpret the experimental phenomena in most metals that with the growth of hardness after heat treatment the scratch friction coefficient (SFC) increases. This interpretation could not be done before. Scratch tests on the surface with or without the coating are discussed. Without the coating the SFC increases due to the decrease of the area with plastic slippage and/or the increase of friction stress during the increase of the yield strength in the material. With a softer substrate the friction stress decreases but the SFC increases, which is caused by the growth of the entire contact area and surface deformation. Conversely, with a stronger substrate the SFC decreases due to an intensified plastic slippage. The obtained results pave a new way to understanding the effects of yield strength on scratch tests, interpret experimental phenomena, and should be helpful for an optimum design in experiments.

Keywords: tribology behavior; yield strength; coating; scratch; finite element method

1 Introduction

There has been an increased interest in the application of surface coatings by changing the surface properties independently of the bulk material [1−4]. Currently scratch tests are widely employed to evaluate the tribological properties of coatings. The finite element method (FEM) becomes an important tool to describe the mechanical responses in the scratch process; it interprets the experimental phenomena; and it further develops experimental, optimum designs. Pioneering 3D FEM simulations of scratch tests, using classic elastoplasticity and Coulomb friction, have been developed for these goals [5−10].

The yield strengths of surface coatings and substrates are very important parameters, and significantly affect the materials' tribological performances. For most metals the hardness increases after heat treatment [11]. It is clear that this increase of hardness or yield strength (yield strength is approximately one third of hardness [12]) leads to a growth in the scratch friction coefficient (SFC); however, a direct explanation for this phenomenon was absent [11]. Previous FEM results based on the traditional Coulomb friction failed to explain it and even displayed an opposite trend; with a growth of yield strength the scratch friction coefficient reduces (e.g., Ref. [8, 10]). The reason was that with the growth of yield strength the deformation of surface material was suppressed, which led to a decrease of the surface deformation friction coefficient (SDFC) and caused a further drop in the SFC [13]. There was a brief attempt to explain this phenomenon in Ref. [13] which combined the Coulomb and plastic friction. One possible reason in Ref. [13] was given for a special case with soft coatings on a very hard substrate, however, it may not be true in other circumstances. As mentioned in Ref. [13], the effects of yield strength need to be reexamined and investigated in a separate

* Corresponding author: Biao FENG, E-mail: biao@lanl.gov

paper. Consequently, one of the goals of this paper is to study the effects of yield strength in the surface coating and further interpret the experimental phenomenon in detail. In addition, the yield strengths in both substrate and coating play an important role in tribological performances of the material surface. Another goal is to investigate the effects of the combined yield strengths of the substrate and coating, which will give completely distinct viewpoints from previous FEM results [5–10, 13].

2 Numerical models

A schematic diagram of a scratch system is shown in Fig. 1. The simulations in this letter follow two continuous steps: first, a vertical external force F_n is exerted along the y-axis to move the spherical indenter towards the coated surface; and second, a horizontal force F_t and a moment M_z are applied to move the indenter in the x-axis direction under a fixed F_n. Such a loading process with a constant vertical force F_n is often used in both experiments and simulations of scratch. All of the results shown in this paper will be for when the indenter slides far away from the initial indentation to avoid the effects of the initial indentation. The moment M_z along the z-axis is necessary to keep the indenter from rotating and was often neglected in schematic diagrams in previous literature. As stated in Ref. [7, 9], it is generally accepted that the scratch test is suitable for coatings with the thickness ranging from 0.1 to 20 μm, which covers a large number of engineering applications. The thickness of the coating and substrate is 5 μm and 35 μm respectively, and the radius of the spherical indenter is 200 μm. The width and length of the coating and substrate are not important parameters as long as they are large enough to exclude the boundary effects. Applications of the results and discussions in this paper are not limited to the current sizes in Fig. 1. If the size of such a scratch system was multiplied by n, then the stress distribution would be the same pattern as the current one if the applied normal force was changed from F_n to $n^2 \cdot F_n$ and the indenter moved horizontally along the x-axis.

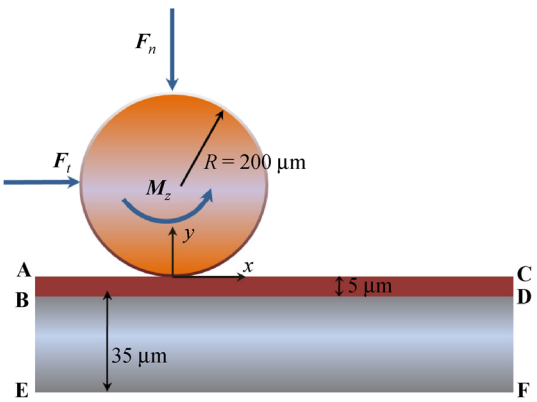

Fig. 1 Schematic representation of the scratch system including an indenter, a thin coating, and a substrate. The boundary EF is fixed during scratch tests.

The indenter is reasonably approximated to be a rigid body. The deformations of the coating and substrate are described by the position vector of the particle in the deformed state $\boldsymbol{r} = \boldsymbol{r}(\boldsymbol{r}_0, t)$, which is a function of its initial position vector $\boldsymbol{r}_0$ in the undeformed configuration and time t. The multiplicative decomposition of the deformation gradient $\boldsymbol{F} = \partial \boldsymbol{r} / \partial \boldsymbol{r}_0 = \boldsymbol{V}_\mathrm{e} \cdot \boldsymbol{F}_\mathrm{p}$ into symmetric elastic stretch tensor $\boldsymbol{V}_\mathrm{e}$ and plastic $\boldsymbol{F}_\mathrm{p}$ contributions is used. While we utilize the small elastic strain assumption: $\boldsymbol{\varepsilon}_\mathrm{e} = \boldsymbol{V}_\mathrm{e} - \boldsymbol{I}$ ($\boldsymbol{I}$ is the second-rank unit tensor), plastic strains and material rotations could be large. A total system of equations for the problem of linearly-elastic, perfectly-plastic flow in the coating and substrate is used as follows:

The deformation rate $\boldsymbol{d} = (\dot{\boldsymbol{F}} \cdot \boldsymbol{F}^{-1})_\mathrm{s}$ is decomposed into elastic (subscript e) and plastic (subscript p) components:

$$\boldsymbol{d} = \overset{\nabla}{\boldsymbol{\varepsilon}}_\mathrm{e} + \boldsymbol{d}_p \tag{1}$$

Hooke's law for volumetric and deviatoric parts of the Cauchy stress $\boldsymbol{T}$:

$$p = -\frac{\sigma_{xx} + \sigma_{yy} + \sigma_{zz}}{3} = -K\varepsilon_\mathrm{v}; \quad \boldsymbol{s} = 2G\, dev\boldsymbol{\varepsilon}_\mathrm{e} \tag{2}$$

Von Mises yield condition:

$$\sigma_i = \left(\frac{3}{2}\boldsymbol{s} : \boldsymbol{s}\right)^{0.5} \leqslant \sigma_y \tag{3}$$

In the elastic region:

$$\sigma_i < \sigma_y \rightarrow \boldsymbol{d}_\mathrm{p} = 0 \tag{4}$$

Plastic flow rule in the plastic region:

$$\sigma_i = \sigma_y \rightarrow \boldsymbol{d}_{\mathrm{p}} = \lambda \boldsymbol{s}\,; \quad \lambda \geqslant 0 \tag{5}$$

Equilibrium equation:

$$\nabla \cdot \boldsymbol{T} = 0 \tag{6}$$

where $\overset{\nabla}{\boldsymbol{\varepsilon}}_{\mathrm{e}}$ is the Jaumann objective time derivative of the elastic strain; p is the pressure; $\boldsymbol{s}$ is the deviator of the Cauchy stress tensor $\boldsymbol{T}$, $\boldsymbol{s} = dev\boldsymbol{T}$; ε_{v} is the elastic volumetric strain; K and G are the bulk and shear moduli respectively; σ_i is the effective stress; σ_y is material yield strength; and the parameter λ is iteratively updated by satisfaction of the von Mises yield criteria in Eq. (3). Material parameters (K, G, and σ_y) have different values for the coating and the substrate.

Similar to pioneering results [5–10, 13], the size effects in Ref. [14, 15] are not considered. The following material properties were used for the metallic coatings [16]: yield strength $\sigma_y = 234$ MPa, Young's modulus $E = 74$ GPa, $v = 0.3$, and Coulomb friction coefficient $\mu = 0.3$. In this paper, to study the effects of yield strength σ_y on coatings and substrates, we will keep the same and constant elastic properties for the coating and substrate, and vary σ_y to different values.

Using the finite element code ABAQUS 6.11, a 3D scratch process was modeled and simulated. The traditional Coulomb friction was utilized in previous FEM simulations on scratch [5–10], and admits that the relative slippage on a contact surface starts when the magnitude of the friction stress vector reaches the critical value $\mu\sigma_{\mathrm{n}}$, where σ_{n} is the normal contact pressure and μ is the traditional friction coefficient. However, for elastoplastic materials the magnitude of the friction stress is limited by shear yield strength $\tau_y = \sigma_y / \sqrt{3}$, where the von Mises yield condition is used for the materials. When friction stress reaches τ_y and is unable to increase, the material loses resistance of complete cohesion, which can initiate sliding [17–22]. This type of slippage and friction is called plastic slippage and plastic friction. During scratch the plastic friction is dominated in many cases especially for soft coating [13]. In this paper a combined Coulomb and plastic friction will be used between the indenter and coating surface, in which the sliding on the contact surface can take place when friction stress reaches a critical value $\tau_{\mathrm{crit}} = \min(\mu\sigma_{\mathrm{n}}, \tau_y)$ [17–22]. In addition, a complete cohesion is used on the contact surface between the coating and substrate.

There are two main friction coefficients. One is the scratch friction coefficient (SFC) μ_s, which is the ratio of tangential and normal resultant forces $\mu_s = F_t / F_n$ (see Fig. 1). The other is the Coulomb friction coefficient (CFC) μ, which is caused by the asperity of the contact pair and is equal to the ratio of the local friction stress and normal contact stress $\mu = \tau / \sigma_{\mathrm{n}}$ when the contact pair is under Coulomb slippage instead of plastic slippage.

3 Numerical results and discussion

First, the simplest case for scratch without a coating in Figs. 2 and 3 will be discussed. In this paper "without coating" means that in Fig. 1 the material properties of substrates are the same with the coating properties. The vertical resultant force $F_n = 0.8$ N will be used in all models. Due to the symmetry in the geometry and loading in Fig. 1, half of the structure will be used in our simulation and results. The symmetry plane is localized at the $z = 0$ plane. Figure 2 shows the distributions of the normal contact stress and the magnitude of the friction stress in one half of the contact surface from the vertical view (see the coordinate system in Fig. 2, and the symmetry plane $z = 0$ goes through the bottom boundary of each from Fig. 2(a) to 2(f)).

With a growth of the yield strength σ_y the contact size l_0 reduces due to the material hardening in Figs. 2(a)–2(c), and the SFC μ_s increases in Fig. 3, which is consistent with experimental observations [11]. The morphology of the contact surface in the elastoplastic material is the same with the surface of the spherical, rigid indenter. With the increase/decrease of the contact surface area in Fig. 2, the indentation depth d will also increase/decrease in Fig. 3. When friction stress reaches yield strength in shear $|\boldsymbol{\tau}| = \tau_y$, the slippage is plastic-slippage controlled. In Figs. 2(d), 2(e), and 2(f), the yield strength in shear τ_y of the material is 135.1, 192.8, and 250.6 MPa respectively and it is noted that in the most contact area the friction stress $|\boldsymbol{\tau}|$ in Figs. 2(d)–2(f) reaches the corresponding yield strength τ_y. Therefore plastic slippage governs at the contact surfaces in Figs. 2(d)–2(f), while the indentation depth is around or less than 1 μm which is not large. l_1 in

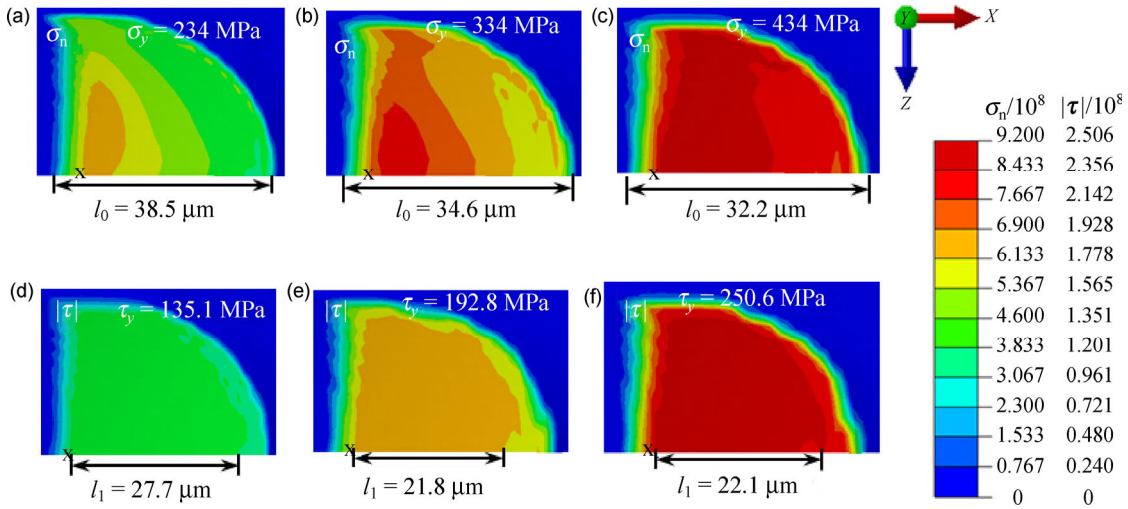

Fig. 2 Distributions of the normal contact pressure σ_n and magnitude of friction stress $|\boldsymbol{\tau}|$ on the contact surface during scratch under axial force $F_n = 0.8$ N, with a growth of yield strength σ_y or τ_y ($\tau_y = \sigma_y/\sqrt{3}$). The material properties of the coating and substrate are the same. The location of indenter tip is marked by a small x.

Figs. 2(d)–2(f) is a length parameter to represent the size of an area with plastic slippage. Material hardening occurs when an increase of the yield strength suppresses the deformation of materials and causes stress concentration. Consequently there is a much larger normal contact stress in Fig. 2(c) than in Fig. 2(a) or 2(b). The SCF $\mu_s = F_t/F_n$ in Fig. 3 is determined by the horizontal external force F_t due to a fixed normal external force F_n as 0.8 N, and the horizontal force F_t is the integral of the components of the normal stress and friction stress along the x-axis with respect to the contact area [13]. In the current cases the indentation depth is around or less than 1 μm which is quite negligible compared to the radius of the indenter $R = 200$ μm, which indicates that the contact surface is almost flat and the component of normal contact stress along the x-axis is very small. Thus the largest contribution of F_t is from the friction stress. When we neglect the bending of coating surface (i.e., the contact surface is close to the flat one), the SFC is approximately equal to $|\boldsymbol{\tau}|/\sigma_n$. The friction stress $|\boldsymbol{\tau}|$ could not increase further and stay as a constant after reaching yield strength in shear ($\tau_y = \sigma_y/\sqrt{3}$), however, the normal stress σ_n can continuously increase. It indicates that the increase of the friction slippage area may cause the reduction of the SFC and the more significant plastic slippage may cause the smaller SFC. In Ref. [13], it is mentioned that the growth of the SFC was

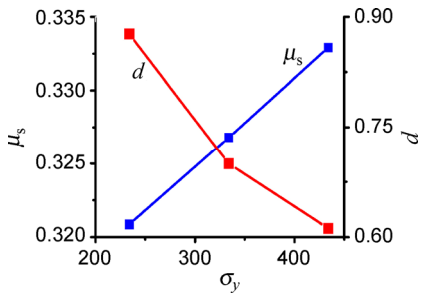

Fig. 3 Scratch friction coefficient μ_s and the indentation depth d with an increase of the yield strength σ_y under axial force $F_n = 0.8$ N in the cases when the substrate has the same material properties as the coating.

caused by a smaller contact area with friction slippage, with a growth of yield strength in the soft surface coating. One can note that this is indeed one of the reasons for SFC growth from Fig. 2(d) to Fig. 2(e), and the other reason is that the rate of growth of friction stress causing an increase in F_t surpasses the rate of the decreasing contact surface causing a drop in F_t. Obviously, the smaller area of plastic slippage in Ref. [13] with a larger yield strength in material is not the reason for the increase in the SFC from Fig. 2(e) to Fig. 2(f). One can find that the areas with plastic slippage in Figs. 2(e) and 2(f) are very comparable. Although the critical friction stress τ_y (when $\tau_y \leqslant \mu\sigma_n$) increases from 192.8 MPa to 250.6 MPa and becomes more difficult to reach on the contact surface, the stress concentration for the material with high yield

strength causes a faster growth of the friction stress, which causes that there is a similar area with plastic slippage in Figs. 2(e) and 2(f). The growth of the SFC is caused by the increasing friction stress rather than a smaller area with plastic slippage in this case.

We will discuss the case when the surface coating and substrate have different yield strengths. Figure 4 shows the distributions of the normal contact stress and the magnitude of friction stress on the coating $\sigma_y = 434$ MPa, with a substrate ($\sigma_y = 334$ MPa or 434 MPa). Here, when the coating and substrate with the same yield strength $\sigma_y = 434$ MPa in Figs. 4(b) and 4(d), it is the case for "without coating". In Fig. 4(a) presents a smaller stress concentration than in Fig. 4(b). The deformation of the soft substrate suppresses the stress concentration in the contact surface and causes a slightly larger contact surface in Fig. 4(a). With less stress concentration it is more difficult for the shear stress to reach yield stress in shear, which causes there to be a smaller area in Fig. 4(c) with plastic slippage than in Fig. 4(d). Smaller plastic slippage leads to a larger SFC for the case in Fig. 4(c), which can be seen in Fig. 5(a). One can find that in Fig. 4(d) the shear stress is slightly larger than in the one in Fig. 4(c) in a large area, however the horizontal force F_t (or SFC) is smaller in Fig. 4(d). One reason is that Fig. 4(c) has a slightly larger contact area, which may cause the integral of the friction stress to be a slightly larger than that in Fig. 4(d). The other reason is caused by a slightly larger surface deformation friction coefficient (SDFC) due to larger indentation depth in Fig. 4(a), which enlarges the SFC (see in Ref. [13]). Consequently, if the plastic slippage reduces then the SFC will increase with a soft substrate. Conversely, with a slight stronger substrate ($\sigma_y = 334$ MPa) the plastic slippage in the coating ($\sigma_y = 234$ MPa) due to stress concentration grows and leads to a reduction of the SFC, in comparison with the case without coatings, shown in Fig. 5(a). In addition, Fig. 5(a) presents that with or without a coating the growth of the yield strength in the materials causes an increase of the SFC. Figure 5(b) shows that with a growth of the yield strength of the gasket, the SFC reduces. The reason is that when yield strength increases in the substrates the stress concentration is intensified, which leads to more obvious plastic slippage in the coating surface and a smaller SFC.

4 Conclusions

In summary, a 3D scratch model is proposed to study the effects of yield strengths in both coatings and substrates by using FEM. A combination of Coulomb and plastic friction is applied on the contact surface

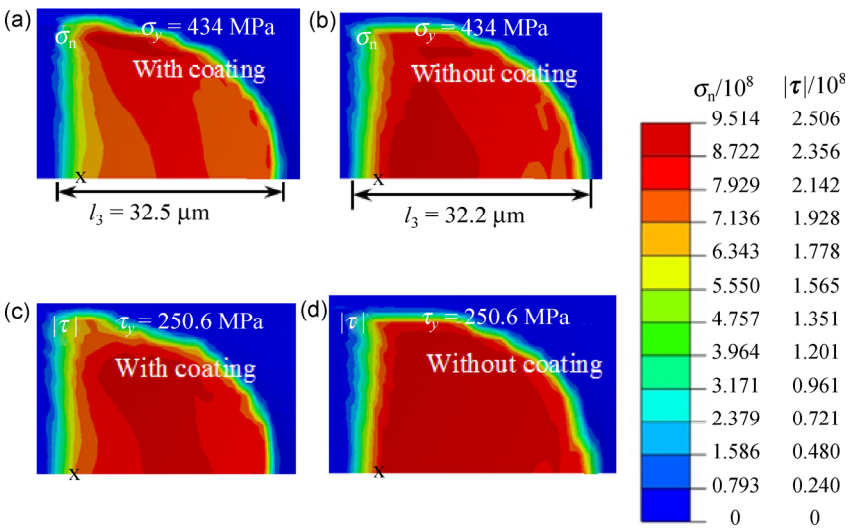

Fig. 4 Distributions of the magnitude of friction stress $|\boldsymbol{\tau}|$ and normal contact pressure σ_n on the contact surface of a coating with $\sigma_y = 434$ MPa during scratch under axial force $F_n = 0.8$ N, with a substrate ($\sigma_y = 334$ MPa in (a) and (c) and $\sigma_y = 434$ MPa in (b) and (d)). In (b) and (d), the yield strengths of coating and substrate are the same, which corresponds to the case: "without coating". The location of indenter tip is marked by a small x.

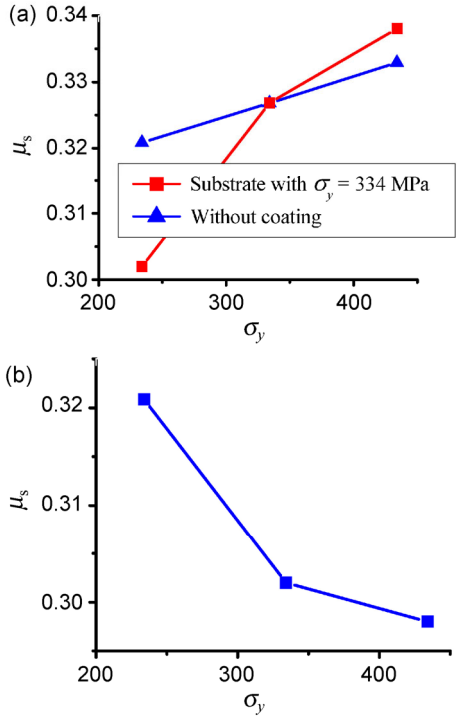

Fig. 5 (a) Variation of the SFC with respect to an increase of the yield strength in the coating with the substrate ($\sigma_y = 334$ MPa) as the red curve, and the substrate with the same yield strength of coating (i.e., "without coating") as the blue curve. (b) Variation of the SFC with a rising yield strength in the substrate for the coating with a constant yield strength $\sigma_y = 234$ MPa .

between the indenter and coating surface. The results show that with and without the coating the increase in the yield strength in the material can cause an increase of the SFC, which is consistent with experimental observations and could not be done before. Without the coating, during an increase of the yield strength in the material, the SFC grows due to a reduction of the area with slippage and/or the increase of the friction stress. When yield strength of the substrate reduces the friction stress may increase but the SFC reduces due to a reduction in contact area and a decrease of the SDFC. Conversely, when yield strength of the substrate grows the stress concentration increases on the coating surface and leads to a more obvious plastic slippage, which causes a reduction of the SFC. The deformation of elastoplasticity also has a significantly effects on the SFC, and especially it determines the SFC before the plastic slippage appears or when the plastic slippage is not dominant in the contact area. Without considering plastic slippage, the effect of the material deformation was widely studied before as in Ref. [5–10]. In the extreme case, when the indenter is deeply inserted into the coating, the effect of sever deformation of contact surface on SFC may be comparable to or even surpass the effect of plastic slippage even though plastic slippage takes place in most of contact region, which requires further study and still stays as a challenge, due to the convergence of simulation and multi-physics such as wear and fracture involved. The obtained results help in better understanding the effects of yield strength on scratch tests and to interpret experimental phenomena, and should be helpful for an optimum design in experiments.

References

[1] Bull S J, Rickerby D S, Jain A. The sliding wear of titanium nitride coatings. *Surf Coat Technol* **41**: 269–283 (1990)

[2] Chalker P R, Bull S J, Rickerby D S. A review of the methods for the evaluation of coating-substrate adhesion. *Mat Sci Eng A-Struct* **140**: 583–592 (1991)

[3] Hogmark S, Jacobson S, Larsson M. Design and evaluation of tribological coatings. *Wear* **246**: 20–33 (2000)

[4] Ivanov V V, Lebedev V A, Pinahin I A. Improving wear resistance of surface by depositing vibrational mechano-chemical MoS_2 coating. *J Frict Wea*r **35**: 339–342 (2014)

[5] Bucaille J L, Gauthier C, Felder E, Schirrer R. The Influence of strain hardening of polymers on the piling-up phenomenon in scratch tests: Experiments and numerical modelling. *Wear* **260**: 803–814 (2006)

[6] Felder E, Bucaille J L, Hochstetter G. Influence of the rheology of polymers on their scratch resistance: Experimental and numerical simulation studies. *Annales De Chimie-Science Des Materiaux* **28**: 15–28 (2003)

[7] Holmberg K, Laukkanen A, Ronkainen H, Wallin K, Varjus S. A Model for Stresses, Crack generation and fracture toughness calculation in scratched TiN-coated steel surfaces. *Wear* **254**: 278–291 (2003)

[8] Jiang H, Lim G T, Reddy J N, Whitcomb J D, Sue H J. Finite element method parametric study on scratch behavior of polymers. *J Polym Sci Pt B-Polym Phys* **45**: 1435–1447 (2007)

[9] Li J, Beres W. Three-dimensional finite element modelling of the scratch test for a TiN coated titanium alloy substrate. *Wear* **260**: 1232–1242 (2006)

[10] Bellemare S C, Dao M, Suresh S. Effects of mechanical properties and surface friction on elasto-plastic sliding contact. *Mech Mater* **40**: 206–219 (2008)

[11] Zhang Z F, Zhang L C, Mai Y W. Particle effects on friction and wear of aluminium matrix composites. *J Mater.Sci* **30**: 5999–6004 (1995)

[12] Hainsworth S V, Soh W C. The effect of the substrate on the mechanical properties of TiN coatings. *Surf Coat Technol* **163**: 515–520 (2003)

[13] Feng B, Chen Z. Tribology behavior during indentation and scratch of thin films on substrates: effects of plastic friction. *AIP Adv* **5**: 057152 (2015)

[14] Chen S H, Feng B, Wei Y G, Wang T C. Prediction of the initial thickness of shear band localization based on a reduced strain gradient theory. *Int. J Solids Struct* **48**: 3099–3111 (2011)

[15] Chen S H, Feng B. Size effect in micro-scale cantilever beam bending. *Acta Mech* **219**: 291–307 (2011)

[16] Ott R D, Blue C A, Santella M L, Blau P J. The influence of a heat treatment on the tribological performance of a high wear resistant high SiAl-Si alloy weld overlay. *Wear* **251**: 868–874 (2001)

[17] Feng B, Levitas V I. Coupled phase transformations and plastic flows under torsion at high pressure in rotational diamond anvil cell: Effect of contact sliding. *J Appl Phys* **114**: 213514 (2013)

[18] Feng B, Levitas V I, Zarechnyy O M. Plastic flows and phase transformations in materials under compression in diamond anvil cell: Effect of contact sliding. *J Appl Phys* **114**: 043506 (2013)

[19] Feng B, Levitas V I, Ma Y. Strain-induced phase transformation under compression in a diamond anvil cell: Simulations of a sample and gasket. *J Appl Phys* **115**: 163509 (2014)

[20] Liu C R, Guo Y B. Finite element analysis of the effect of sequential cuts and tool-chip friction on residual stresses in a machined layer. *Int J Mech Sci* **42**: 1069–1086 (2000)

[21] Zhang H W, Zhang Z, Chen J T. The finite element simulation of the friction stir welding process. *Mat Sci Eng A-Struct* **403**: 340–348 (2005)

[22] Feng B, Levitas V I. Effects of gasket on coupled plastic flow and strain-induced plase transformations under high pressure and large torsion in a rotational diamond anvil cell. *J Appl Phy* **119**: 015902 (2016)

Biao FENG. He received his Master degree from Institute of Mechanics, Chinese Academy of Sciences, Beijing, in 2011. He earned his Ph.D. degree in engineering mechanics from Iowa State University in 2015, and afterwards did his postdoc research there for one year. Biao Feng has been conducting his research at Los Alamos National Laboratory since September 2016. His current research interest is on advanced mechanics of materials under extreme conditions.